Nanoscale

PAPER

View Article Online
View Journal | View Issue

Cite this: *Nanoscale*, 2024, **16**, 9400

Freeze-crosslinking approach for preparing carboxymethyl cellulose nanofiber/zirconium hydrogels as fluoride adsorbents†

Yurina Sekine, *[a] Takuya Nankawa,[b] Tsuyoshi Sugita,[a] Yoshiyasu Nagakawa,[c] Yuki Shibayama,[a] Ryuhei Motokawa[a] and Tomoko Ikeda-Fukazawa[d]

Received 11th April 2024,
Accepted 16th April 2024

DOI: 10.1039/d4nr01572j

rsc.li/nanoscale

Tough carboxymethylcellulose nanofibers (CMF)/zirconium (Zr) hydrogels were easily obtained by a freeze-crosslinking method, where Zr-containing HCl solution was added to frozen CMF sol and the mixture was allowed to thaw. The Zr content of the hydrogels increased with increasing Zr concentration in the initial HCl solution. Furthermore, the mechanical strength increased with increasing Zr content. The Young's modulus value was improved by approximately 6 times compared to the CMF hydrogel without Zr, *i.e.*, from 4.5 kPa to 27.2 kPa. The hydrogel had a porous structure with a pore size of 133 ± 37 μm and a CMF–Zr sheet structure around the pores. The obtained CMF–Zr hydrogel exhibited high adsorptivity for fluoride. The maximum adsorption capacity (Q_{max}) was estimated to be 24.1 mg g^{-1}. This simple gelation method provides useful insights for the development of easy-to-handle hydrogel-based adsorbents.

[a]*Materials Sciences Research Center, Japan Atomic Energy Agency (JAEA), Tokai, Ibaraki 319-1195, Japan. E-mail: sekine.yurina@jaea.go.jp*
[b]*Promotion Office, JAEA, Tokai, Ibaraki 319-1195, Japan*
[c]*Tokyo Metropolitan Industrial Technology Research Institute, Aomi, Koto-ku, Tokyo 135-0064, Japan*
[d]*School of Science and Technology, Meiji University, Kawasaki, Kanagawa 214-8571, Japan*

†Electronic supplementary information (ESI) available. See DOI: **https://doi.org/10.1039/d4nr01572j**

Yurina Sekine

Yurina Sekine is currently an assistant principal researcher at the Japan Atomic Energy Agency (JAEA). She completed her PhD in polymeric biomaterials at the Tokyo Medical and Dental University in 2012. Since then, she has been working as a researcher at JAEA. To expand her skills, she worked as a visiting researcher at the Northwestern University in 2017. She is a recipient of the 2022 Chemical Society of Japan Award for Outstanding Young Women Chemists. Her current research interests include the development of structurally controlled biomass-based hydrogels for advanced environmental cleanup resource recovery, energy conversion, and high-throughput analysis applications.

Introduction

Hydrogels are polymer materials that can hold large amounts of water (>95%) within their crosslinked polymer networks. Recently, the use of hydrogels as adsorbents that allow wastewater to flow inside them and only harmful substances to be adsorbed by the polymer networks has attracted considerable attention.[1,2] The adsorption properties of hydrogels can be tuned by varying the polymer and network structure.[3]

Although numerous adsorbents have been reported to date, such as activated carbon, zeolites, and polymer-based materials, the development of adsorbents that can adsorb anionic substances remains a challenge.[4] Wastewater contains various anions that must be removed, including fluoride, bromate, or arsenic. Cationic adsorbents such as carbonaceous materials,[5] metal-based materials,[6] and ion-exchange resins[7] are useful for removing these anions, but their applicability is limited due to issues such as difficult to handle, high cost, and low sustainability. The development of new types of adsorbents should enable efficient decontamination under diverse environments. The use of zirconium (Zr), which is a non-toxic cationic metal that can form complexes with renewable polymers such as cellulose, represents a promising strategy for realizing versatile and environmentally friendly cationic adsorbents.[8,9] However, it is still necessary to develop Zr-hydrogel composites with sufficient mechanical strength, facile synthesis, easy to handle, and good decontamination performance.

The freeze-crosslinking method is a valuable and extremely simple approach for obtaining high-strength macroporous

hydrogels. High-strength hydrogels based on cellulose[2,10] and poly(vinyl alcohol) (PVA)[11] have been prepared using this method, which involves simply adding a crosslinker solution into frozen polymer sols such as cellulose or PVA and thawing the resulting mixture. Normally, when water containing solutes freezes, the solutes and bound water are not incorporated into the ice crystals and instead form freeze-concentrated layers (FCLs) around them (Fig. S1†).[12] These FCLs have been reported to remain fluid even at around 230 K.[13] Consequently, condensed reactive polymers in the FCLs can react with crosslinkers even in the presence of ice, leading to the formation of unusual ordered network structures.

Such reactions in FCLs may enable the creation of novel functional hydrogel materials. However, there have been very few reports of freeze crosslinking being applied to polymer–metal composites. In this work, we aimed to develop a Zr-containing cellulose-based composite hydrogel featuring high strength and good fluoride adsorption performance using the freeze-crosslinking approach.

Materials and methods

Materials

An aqueous carboxymethyl cellulose nanofiber (CMF) sol (2 wt%, TFo-100002) prepared using a water jet system was purchased from Sugino Machine Limited, Japan.[14] Zirconium chloride oxide octahydrate ($ZrCl_2O{\cdot}8H_2O$), zirconium oxide (ZrO_2), hydrogen chloride (HCl) (1 mol L^{-1}), and fluoride ion standard solution (sodium fluoride (NaF), 1004 mg L^{-1}) were purchased from Fujifilm Wako Pure Chemical Co. Ltd, Japan.

Preparation of hydrogel samples

The CMF-F-Z*x* hydrogels were prepared as follows. First, $ZrCl_2O{\cdot}8H_2O$ was dissolved in HCl solution (1 mol L^{-1}) at x = 0.1, 0.5, 1, or 3 wt% to obtain the desired HCl-Z*x* solutions (where x denotes the $ZrCl_2O{\cdot}8H_2O$ content in wt%). Separately, samples of the CMF sol (2 g, 2 wt%) were frozen in a freezer at 253 K for 12 h. The HCl-Z*x* solutions (2 mL) were then added to the frozen CMF sols. The mixtures were allowed to thaw in a refrigerator at 277 K for 24 h (Fig. 1). The resulting hydrogels were repeatedly washed and then immersed in Milli-Q water for 24 h. CMF-F was prepared by the same procedure but with the omission of $ZrCl_2O{\cdot}8H_2O$ from the HCl solution. CMF-R-Z3 was obtained by gently adding HCl-Zr3 solution (2 mL) onto the CMF sol (2 g) and allowing the sample to stand at room temperature for 24 h. CMF-mix-Z3 was prepared by mixing $ZrCl_2O{\cdot}8H_2O$ (60 mg) with the CMF sol (2 g). Water contents (W) (%) was calculated using the following equation: W (%) = $(W_{sgel} - W_{dgel})/W_{sgel} \times 100$, where W_{sgel} (g) and W_{dgel} (g) denote the weights of the swollen and dried hydrogels prepared by heating at 373 K, respectively. The gelation ratio (R_{gel}) (%) was calculated using the following equation: $R_{gel} = W_{dgel}/W_{ICMF} \times 100$, where W_{ICMF} (g) denotes the weight of CMF in the initial sample and was calculated by multiplying the weight of the initial CMF sol by 0.02 based on its concentration of 2 wt%.

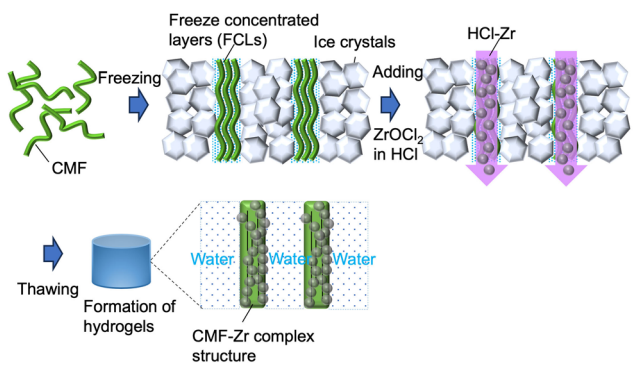

Fig. 1 Schematic illustration of the preparation of CMF-F-Z*x* hydrogels.

Characterization

The compressive strengths of the swollen samples were measured on a texture analyser (TA.XTplus, Stable Micro Systems Co. Ltd, UK). Thermogravimetric (TG), Brunauer–Emmett–Teller (BET), scanning electron microscopy (SEM), X-ray photoelectron spectroscopy (XPS), Fourier-transform infrared (FT-IR) spectroscopy, and powder X-ray diffraction (PXRD) measurements were performed using freeze-dried hydrogel samples. TG tests were carried out using an analyzer (TG-DTA, TG-8120, Rigaku Co., Japan). The specific surface area was measured by using nitrogen at 77 K in a gas sorption system (BELSORP MAXX, MicrotracBEL Corp.). SEM-energy-dispersive X-ray (EDX) images were recorded on a JSM-6010PLUS/LA (JEOL Ltd, Japan). XPS spectra were measured on a spectrometer (Quantes, ULVAC-PHI, Inc., Japan) with Al-K_α radiation (25 W, 15 kV). FT-IR spectra were measured on a spectral reflectometer (FT/IR-6600, JASCO, Japan) equipped with a diffuse reflection unit (DR-81, JASCO). PXRD patterns were acquired on an X-ray diffractometer (MiniFlex600, Rigaku Co. Ltd, Japan) with Cu-K_α radiation. Small-angle neutron scattering (SANS) experiments were performed for swollen hydrogel samples using a SANS diffractometer with sample-to-detector distance of 2 and 10 m, SANS-J[15] at the research reactor, JRR-3. The details of characterization were described in the ESI.†

Sorption tests

Adsorption measurements were performed using freeze-dried samples and aqueous solutions of NaF at a concentration of 1–20 mmol L^{-1}. The sample (35 mg) was added to the aqueous fluoride solution (7 mL) and the resulting mixture was stirred without pH control for 0.25 to 24 hours. The supernatant was removed and its fluoride concentration was determined by ion chromatography on a Dionex ICS-2100 system (Thermo Fisher Scientific, Waltham, MA, USA) equipped with a Dionex IonPac AS11-HC column for elemental separation. KOH (10 mmol L^{-1}) was used as the eluent. The removal efficiency (R_{eff}) was calculated using the following equation: $R_{eff} = (C_i - C_t)/C_i \times 100$, where C_i and C_t (mg L^{-1}) denote the initial fluoride concen-

tration in the aqueous solution and the fluoride concentration after reaction time t, respectively.

Results and discussion

Preparation of freeze-crosslinked CMF-F-Zx hydrogels

The CMF-F-Zx hydrogels were free standing and did not break during compression under a load of 100 g (Fig. 2(a) and S2†). By contrast, mixing the CMF sol and an aqueous solution of HCl-Z3 at room temperature afforded a free-standing but fragile hydrogel (CMF-R-Z3), while mixing the CMF sol and $ZrCl_2O{\cdot}8H_2O$ powder gave a misshapen and fragile hydrogel (CMF-mix-Z3) (Fig. 2(a)). The results demonstrated that freeze crosslinking between CMF and HCl-Zr provided free-standing hydrogels with satisfactory mechanical properties.

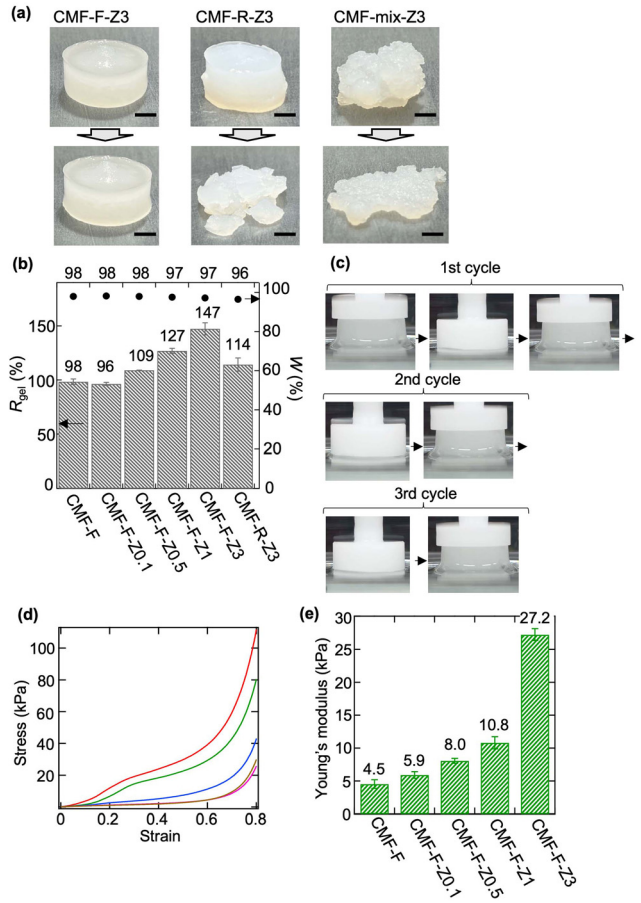

Fig. 2 (a) Photographs of the CMF-F-Z3, CMF-R-Z3, and CMF-mix-Z3 samples (top: initial, bottom: after compression under a load of 100 g). The scale bars represent 5 mm. (b) R_{eff} (%) and W (%) values for CMF-F, CMF-F-Zx (x = 0.1, 0.5, 1, or 3), and CMF-R-Z3. The bar graph and filled circles represent R_{gel} and W, respectively. (c) Photographs of CMF-F-Z3 during cyclic compression tests for three cycles. (d) Stress–strain curves for CMF-F (brown), CMF-F-Z0.1 (pink), CMF-F-Z0.5 (blue), CMF-F-Z1 (green), CMF-F-Z3 (red). (e) Young's moduli of CMF-F and the CMF-F-Zx hydrogels.

Effects of Zr on properties of CMF-F-Zx hydrogels

The values of R_{gel} (%) and W (%) of the CMF-F-Zx hydrogels (x = 0.1, 0.5, 1, or 3) are shown in Fig. 2(b). The R_{gel} and W values of CMF-R-Z3 and CMF-F are also shown for comparison. R_{gel} was calculated using the weight of CMF in the initial sol sample (2 wt%); thus, values above 100% mean that the sample contained Zr. The R_{gel} values of the CMF-F-Zx hydrogels increased with increasing x from 98% for CMF-F to 147% for CMF-F-Z3. The W values (*ca.* 97%) were similar irrespective of x. These results indicate that all of the CMF-F-Zx hydrogels had a high-water content and the Zr content increased with increasing x.

The CMF-F-Zx hydrogels exhibited mechanical toughness, and the mechanical strength increased with increasing Zr content. CMF-F-Z3 displayed high compressive recoverability during cyclic compression tests (Fig. 2(c)). The stress–strain curves of CMF-F and the CMF-F-Zx samples are plotted in Fig. 2(d). The stress–strain curve of CMF-F-Z0.1 was similar to that of CMF-F, but the curve shape changed with x. Both CMF-F-Z1 and CMF-F-Z3 exhibited a yielding point at a strain of approximately 0.3, indicating characteristic plastic deformation behaviour.[16] Similar behaviour has been observed in most tough hydrogels composed of polymers and metals.[16] The Young's modulus increased with increasing x from 4.5 kPa for CMF-F to 27.2 kPa for CMF-F-Z3 (Fig. 2(e)). Thus, complexation between CMF and Zr during freeze crosslinking significantly enhanced the mechanical properties of the CMF-F-Zx hydrogels.

Effects of Zr on structures of CMF-F-Zx hydrogels

SEM images of CMF-F-Z3 revealed a porous structure with a pore diameter of 133 ± 37 μm and a sheet structure around the pores (Fig. 3(a)), similar to the results observed for CMF-F (Fig. S3†).[17] A mottled structure was also apparent on the surface of the sheet structure. Similar structures were pre-

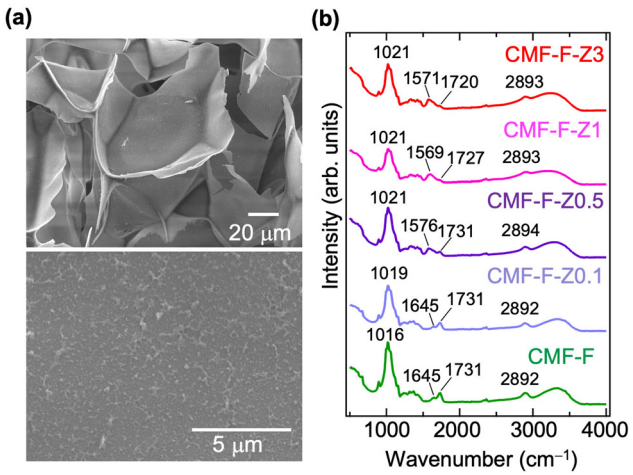

Fig. 3 (a) SEM images of the freeze-dried CMF-F-Z3 (upper) and the corresponding magnified image (bottom). (b) IR spectra of freeze-dried CMF-F and CMF-F-Zx.

viously observed in cellulose-Zr complex materials.[9,18] EDX analysis indicated that CMF-F-Z3 was composed of C (43%), O (33%), Zr (17%), and Cl (7%), and the Zr : Cl ratio of the CMF-F-Z*x* hydrogels increased with increasing *x* (Fig. S3†). Zr was observed throughout the entire structure (Fig. S3†). The specific surface area of CMF-F-Z3 was estimated to be 3.33 m^2 g^{-1} by BET method, which was larger than that of CMF-F (2.21 m^2 g^{-1}). Those results indicate that the freeze-crosslinking approach resulted in the introduction of Zr into the CMF hydrogel.

Fig. 3(b) shows the FT-IR spectra of freeze-dried CMF-F and the CMF-F-Z*x* hydrogels (*x* = 0.1, 0.5, 1, or 3) in the 500–4000 cm^{-1} range. All of the spectra exhibited several characteristic peaks originating from CMF, including those corresponding to skeletal vibrations (1016 cm^{-1}), C=O stretching (1645 and 1731 cm^{-1}), C–H stretching (2892 cm^{-1}), and O–H stretching (3050–3600 cm^{-1}), as shown in the spectrum of CMF-F.[17] In the CMF-F-Z*x* spectra, the C=O stretching modes shifted to lower wavenumber with increasing *x* (*e.g.*, from 1645 and 1731 cm^{-1} for *x* = 0.1 to 1571 and 1720 cm^{-1} for *x* = 3), which was ascribed to the interaction between Zr and COOH moieties. Similar peak shifts have been observed in other cellulose-Zr complex materials.[8,9,18] In addition, the O–H band became broader with increasing *x*. Broader O–H bands can result from hydrogen bonds in various conditions.[19] This suggests that Zr also interacted with O–H in the CMF-F-Z*x* hydrogels.

Fig. 4(a) presents the SANS patterns of CMF-F, CMF-F-Z3, CMF-R-Z3, and CMF-mix-Z3 under wet conditions in the scattering vector (*Q*) range from 0.03 to 3 nm^{-1}. In the case of CMF-F, a clear hump was observed at *Q* = 0.2 nm^{-1}, indicating that the hydrogel had a specific structure on the scale of tens of nanometres. The *d* spacing was estimated as 31 nm. Similar humps have been observed for freeze-crosslinked cellulose nanofiber hydrogels,[2] as well as for water-dispersed cellulose microfibrils at high concentrations.[20] These may be attributable to the self-ordering of cellulose molecules. A similar hump was also observed for CMF-F-Z3, but its intensity was lower than that for CMF-F. These findings suggest that the degree of cellulose ordering decreased upon permeation of the Zr from the FCLs into the CMF structure to form a more complex structure. A significant decrease in the intensities of the Bragg diffraction peaks from cellulose was also observed in the PXRD pattern of CMF-F-Z3 (Fig. S4†). In the SANS pattern of CMF-R-Z3, a slight hump was observed at around *Q* = 0.15 nm^{-1}, which may be attributable to the crosslinking of CMF under the acidic conditions. The SANS pattern of CMF-mix-Z3 exhibited no discernible hump in the examined *Q* range, indicating that the simple mixing of CMF and Zr afforded an inhomogeneous CMF-Zr complex. These results show that CMF-F-Z3 had a similar structure to CMF-F, albeit with a lower degree of cellulose ordering. This complex structure of CMF and Zr likely accounted for the high mechanical strength.

The full scale of XPS curve of CMF-F-Z3, ZrO_2, and $ZrCl_2O{\cdot}8H_2O$ were measured (Fig. S5†). In the spectrum of CMF-F-Z3, some peaks corresponding to Zr 3s at ~434 eV, Zr 3p at ~348 eV and 334 eV, and Zr 3d at ~184 eV were shown. The XPS Zr 3d spectrum for CMF-F-Z3 have two peaks at 183.23 eV and 185.53 eV, corresponding to the Zr $3d_{5/2}$ and Zr $3d_{3/2}$.[9,21–23] The peak positions were ~0.2 eV lower than those of $ZrCl_2O{\cdot}8H_2O$ (183.4 eV and 185.8 eV) and ~0.5 eV higher than ZrO_2 (182.7 eV and 185 eV). The shape of the Zr 3d spectrum was similar to that of $ZrCl_2O{\cdot}8H_2O$ (Fig. 4(b)). This suggests Zr in CMF-F-Z3 exists as Zr(IV) and bonds to O and Cl.

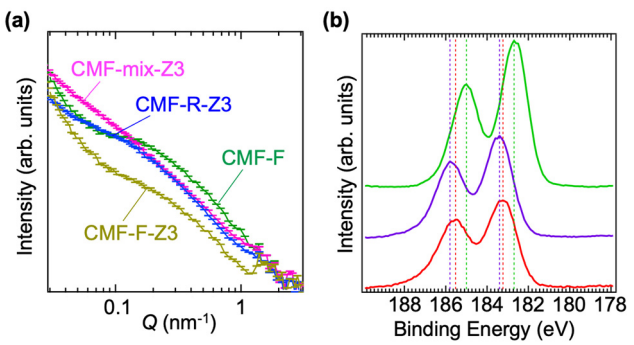

Fig. 4 (a) SANS patterns of CMF-F (green), CMF-F-Z3 (yellow), CMF-R-Z3 (purple), and CMF-mix-Z3 (pink), respectively. (b) XPS spectra of Zr 3d in CMF-F-Z3 (red), $ZrCl_2O{\cdot}8H_2O$ (purple), ZrO_2 (green). The red, purple, and green dashed lines represent the peak positions of CMF-F-Z3, $ZrCl_2O{\cdot}8H_2O$, and ZrO_2, respectively.

Fluoride adsorptivity of CMF-F-Z*x* hydrogels

The fluoride adsorption performance of the CMF-F-Z*x* hydrogels was investigated by conducting sorption tests using fluoride solution at approximately pH 7. Fig. 5(a) shows the R_{eff} of the samples. CMF-F did not adsorb fluoride ions. By contrast, the R_{eff} values of the CMF-F-Z*x* hydrogels increased with increasing *x* from 0% for CMF-F-Z0.1 to 81% for CMF-F-Z3. Thus, CMF-F-Z3 exhibited the highest adsorptivity for fluoride ions. In addition, CMF-F-Z3 did not break when the liquid is pushed out after adsorbing fluoride ions (Fig. 5(b)), enabling convenient removal and volume reduction of the spent adsorbent.

After the adsorption test, we confirmed the fluoride ion concentrations of the remaining solution and the solution squeezed out from the CMF-F-Z3 hydrogel were same. This indicates that the fluorine solution efficiently penetrated inside the CMF-F-Z3 hydrogel, and Zr was immobilized and adsorbed on the skeleton structure. Fluorine ions are thought to be immobilized through electrostatic interaction and ion exchange.[9,23]

The effect of contact time on the adsorption performance of the CMF-F-Z3 was examined by measuring the equilibrium adsorption capacity (Q_e) with reaction time. The adsorption reaction of CMF-F-Z3 for fluoride ions reached equilibrium after 4 hours. The adsorption behavior is similar to that of other porous adsorbents.[24] Based on the result, we measured the maximum adsorption capacity (Q_{max}) by measuring concentrations of fluoride ions after reaction time for 24 hours. The adsorption isotherm of CMF-F-Z3 was fitted using the Langmuir isotherm model with the fitting parameters listed in Table S1† as shown in Fig. 5(d).[25] According to the Langmuir

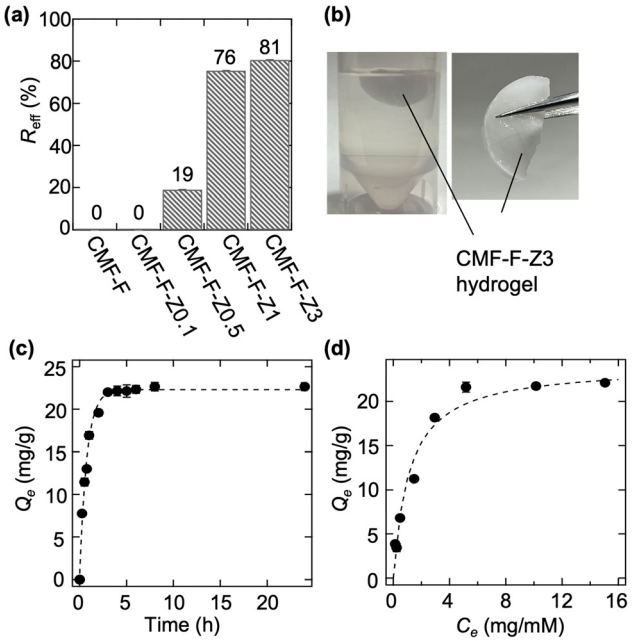

Fig. 5 (a) R_{eff} values for CMF-F and CMF-F-Z*x* (*x* = 0.1, 0.5, 1, or 3) in an aqueous solution of NaF (1 mmol L^{-1}). (b) Photographs of CMF-F-Z3 during (left) and after (right) immersion in aqueous solution. (c) Q_e values of CMF-F-Z3 in an aqueous solution of NaF (10 mmol L^{-1}) with reaction time. (d) Fluoride adsorption isotherm analysis for CMF-F-Z3. The dashed line represents the fitting curve obtained using the Langmuir model.

isotherm model, the Q_{max} was estimated to be 24.1 mg g^{-1}. TG tests showed that the freeze-dried CMF-F-Z3 contained approximately 14.5% water (Fig. S6†). Thus, the value of Q_{max} was calculated considering the amount of water in the sample. The value of Q_{max} is similar to that of most previously developed fluoride adsorbents.[26] The Q_{max} value of ZrO_2 was also examined for comparison. The Q_{max} of $ZrCl_2O{\cdot}8H_2O$ could not be examined because it was dissolved in the reaction solution. The Q_{max} value of ZrO_2 (Q_{max} = 1.5 mg g^{-1}) was much lower than that of CMF-F-Z3.

The recovery of adsorbed metal and reusability of adsorbents are important parameters for building sustainable systems. The fluoride ions desorption reaction of CMF-F-Z3 was examined.[27] Fluoride adsorbed CMF-F-Z3 was prepared by stirring CMF-F-Z3 in a fluoride solution (10 mmol L^{-1}) for 24 hours. Then, the sample was emersed in an aqueous solution of ammonium hydroxide (NH_4OH) (5.6 mol L^{-1}) or HCl (0.1 mol L^{-1}) for 24 hours. 95% and 75% of the adsorbed fluoride ions were released from CMF-F-Z3 after the reaction, respectively. The reused CMF-F-Z3 adsorbed only approximately 20% of fluoride ions. Further research is needed on the reusability of the adsorbent.

These results demonstrate that CMF-F-Z*x* has the advantages of facile preparation, sufficient strength for convenient handling, and has a high potential to become a good fluoride adsorbent. It may also be possible to further improve the adsorption performance by tuning the network structure and Zr content.

Conclusions

CMF-F-Z*x* hydrogels with sufficient mechanical strength were prepared by using freeze cross-linking reactions between CMF and Zr in FCLs. The developed CMF-F-Z*x* exhibited sufficient adsorptivity for fluoride. This study demonstrated that the freeze cross-linking method allows for facile and low-cost preparation of Zr-hydrogel composites that have a high potential as fluoride adsorbents.

Author contributions

Yurina Sekine: conceptualization, methodology, visualization, investigation, validation, formal analysis, data curation, writing – original draft, writing – review & editing, supervision, project administration, funding acquisition. Takuya Nankawa: methodology, visualization, investigation, formal analysis, data curation, writing – original draft, supervision. Tsuyoshi Sugita: formal analysis, data curation, investigation. Yuki Shibayama: formal analysis, data curation. Yoshiyasu Nagakawa: formal analysis, data curation. Ryuhei Motokawa: formal analysis, data curation. Tomoko Ikeda-Fukazawa: formal analysis, data curation.

Conflicts of interest

There are no conflicts to declare.

Acknowledgements

This work was supported by JSPS KAKENHI (grants 21K04949 to T. N. and Y. S., 21H01151 to T. F. and Y. S., 21K07992 to Y. N. and Y. S., and 22K05205 to T. S. and Y. S.). Access to the experiment at the SANS-J (C3-2) was provided by the JRR-3 with the approval of JAEA (proposal 2023-D775). This work was supported by "Advanced Research Infrastructure for Materials and Nanotechnology in Japan (ARIM)" of the Ministry of Education, Culture, Sports, Science and Technology (MEXT). Proposal number is JPMXP1223NM0183. We are grateful to Dr Hideyuki Yasufuku of NIMS for supporting the XPS experiments. We would like to thank ThinkSCIENCE for the English language review.

References

1 F. Zhao, Y. Guo, X. Zhou, W. Shi and G. Yu, *Nat. Rev. Mater.*, 2020, **5**, 388–401.
2 Y. Sekine, T. Nankawa, K. Hiroi, Y. Oba, Y. Nagakawa, T. Sugita, Y. Shibayama and T. Ikeda-Fukazawa, *Carbohydr. Polym.*, 2024, **327**, 121538.
3 V. Van Tran, D. Park and Y. C. Lee, *Environ. Sci. Pollut. Res. Int.*, 2018, **25**, 24569–24599.

4 L. N. Pincus, H. E. Rudel, P. V. Petrovic, S. Gupta, P. Westerhoff, C. L. Muhich and J. B. Zimmerman, *Environ. Sci. Technol.*, 2020, **54**, 9769–9790.
5 M. M. Hassan and C. M. Carr, *Chemosphere*, 2021, **265**, 129087.
6 E. Kumar, A. Bhatnagar, W. Hogland, M. Marques and M. Sillanpää, *Chem. Eng. J.*, 2014, **241**, 443–456.
7 S. Meenakshi and N. Viswanathan, *J. Colloid Interface Sci.*, 2007, **308**, 438–450.
8 Y. Ibrahim, E. Abdulkarem, V. Naddeo, F. Banat and S. W. Hasan, *Sci. Total Environ.*, 2019, **690**, 167–180.
9 J. Wang, X. Lin, X. Luo and Y. Long, *Chem. Eng. J.*, 2014, **252**, 415–422.
10 Y. Sekine, T. Nankawa, S. Yunoki, T. Sugita, H. Nakagawa and T. Yamada, *ACS Appl. Polym. Mater.*, 2020, **2**, 5482–5491.
11 M. Hua, S. Wu, Y. Ma, Y. Zhao, Z. Chen, I. Frenkel, J. Strzalka, H. Zhou, X. Zhu and X. He, *Nature*, 2021, **590**, 594–599.
12 Y. Sekine and T. Nankawa, *Bull. Chem. Soc. Jpn.*, 2023, **96**, 1150–1155.
13 H. O'Neill, S. V. Pingali, L. Petridis, J. He, E. Mamontov, L. Hong, V. Urban, B. Evans, P. Langan, J. C. Smith and B. H. Davison, *Sci. Rep.*, 2017, **7**, 11840.
14 Y. Watanabe, S. Kitamura, K. Kawasaki, T. Kato, K. Uegaki, K. Ogura and K. Ishikawa, *Biopolymers*, 2011, **95**, 833–839.
15 T. Kumada, R. Motokawa, Y. Oba, H. Nakagawa, Y. Sekine, C. Micheau, Y. Ueda, T. Sugita, A. Birumachi, M. Sasaki, K. Hiroi and H. Iwase, *J. Appl. Crystallogr.*, 2023, **56**, 1776–1783.
16 M. X. Wang, C. H. Yang, Z. Q. Liu, J. Zhou, F. Xu, Z. Suo, J. H. Yang and Y. M. Chen, *Macromol. Rapid Commun.*, 2015, **36**, 465–471.
17 D. Miura, Y. Sekine, T. Nankawa, T. Sugita, Y. Oba, K. Hiroi and T. Ohzawa, *Carbohydr. Polym. Technol. Appl.*, 2022, **4**, 100251.
18 Z. Chang, S. Li, L. Sun, C. Ding, X. An and X. Qian, *Cellulose*, 2019, **26**, 6739–6754.
19 Y. Sekine and T. Ikeda-Fukazawa, *J. Chem. Phys.*, 2009, **130**, 034501.
20 W. J. Orts, L. Godbout, R. H. Marchessault and J. F. Revol, *Macromolecules*, 1998, **31**, 5717–5725.
21 A. Contreras-Ramirez, B. E. Tomlin, G. S. Day, A. Clearfield and H. Zhou, *Chem. – Eur. J.*, 2020, **26**, 6185–6194.
22 C. Sleigh, A. P. Pijpers, A. Jaspers, B. Coussens and R. J. Meier, *J. Electron Spectrosc. Relat. Phenom.*, 1996, **77**, 41–57.
23 X. Dou, D. Mohan, C. U. Pittman Jr. and S. Yang, *Chem. Eng. J.*, 2012, **198–199**, 236–245.
24 T. Nankawa, Y. Sekine and T. Yamada, *Bull. Chem. Soc. Jpn.*, 2022, **95**, 825–829.
25 I. Langmuir, *J. Am. Chem. Soc.*, 2002, **40**, 1361–1403.
26 W.-Z. Gai and Z.-Y. Deng, *Environ. Sci.: Water Res. Technol.*, 2021, **7**, 1362–1386.
27 X. Liao and B. Shi, *Environ. Sci. Technol.*, 2005, **39**, 4628–4632.